PNAS RESEARCH ARTICLE | GENETICS OPEN ACCESS

Mitochondrial mutations alter endurance exercise response and determinants in mice

Patrick M. Schaefer[a], Komal Rathi[b], Arrienne Butic[a], Wendy Tan[a], Katherine Mitchell[a], and Douglas C. Wallace[a,c,1]

Contributed by Douglas Wallace; received January 21, 2022; accepted February 25, 2022; reviewed by Bret Goodpaster, Laurie Goodyear, Pablo Garcia-Roves, and Dan Cooper

Primary mitochondrial diseases (PMDs) are a heterogeneous group of metabolic disorders that can be caused by hundreds of mutations in both mitochondrial DNA (mtDNA) and nuclear DNA (nDNA) genes. Current therapeutic approaches are limited, although one approach has been exercise training. Endurance exercise is known to improve mitochondrial function in heathy subjects and reduce risk for secondary metabolic disorders such as diabetes or neurodegenerative disorders. However, in PMDs the benefit of endurance exercise is unclear, and exercise might be beneficial for some mitochondrial disorders but contraindicated in others. Here we investigate the effect of an endurance exercise regimen in mouse models for PMDs harboring distinct mitochondrial mutations. We show that while an mtDNA ND6 mutation in complex I demonstrated improvement in response to exercise, mice with a CO1 mutation affecting complex IV showed significantly fewer positive effects, and mice with an ND5 complex I mutation did not respond to exercise at all. For mice deficient in the nDNA adenine nucleotide translocase 1 (Ant1), endurance exercise actually worsened the dilated cardiomyopathy. Correlating the gene expression profile of skeletal muscle and heart with the physiologic exercise response identified oxidative phosphorylation, amino acid metabolism, matrisome (extracellular matrix [ECM]) structure, and cell cycle regulation as key pathways in the exercise response. This emphasizes the crucial role of mitochondria in determining the exercise capacity and exercise response. Consequently, the benefit of endurance exercise in PMDs strongly depends on the underlying mutation, although our results suggest a general beneficial effect.

mitochondrial disease | endurance exercise | skeletal muscle adaption

Mitochondria generate most of the cellular energy and are critical in regulating cellular reactive oxygen species (ROS) production, pH and Ca^{2+} levels, apoptotic initiation, redox state, and intracellular signaling (1). Mitochondria are assembled from genes coded in both the mitochondrial DNA (mtDNA) and the nuclear DNA (nDNA). The mtDNA codes for 13 crucial polypeptides of mitochondrial oxidative phosphorylation (OxPhos), while the nDNA codes for all of the remaining ~1,500 mitochondrial genes. Mutations in these mitochondrial genes can result in primary mitochondrial diseases (PMDs) that can be characterized by fatigue, myopathy, cardiomyopathy, and neuropsychiatric disorders (2). However, the phenotype and severity vary due to the multitude of different nDNA and mtDNA mutations.

Patients homoplasmic for the mtDNA *ND6* m.14600G > A mutation (Proline codon 25 to Leucine, P25L) manifest with progressive encephalopathy and Leigh syndrome resulting in childhood death (3), while heteroplasmic patients show early adulthood optic atrophy and cerebellar ataxia (3). Mice harboring the analogous mtDNA *ND6* m.13997G > A (P25L, $ND6^{P25L}$) mutation present with retinal dysfunction and optic nerve pathology (4) as well as autism spectrum disorder (5). Complex I activity is reduced 50 to 60% in the *ND6*-mutant mice, resulting in a more reduced NAD/NADH ratio (6), an increased number of abnormal mitochondria, but no decline in ATP levels (4). Mice harboring a homoplasmic mtDNA *CO1 m.*6589T > C missense mutation (V421A, $CO1^{V421A}$) in the cytochrome *c* oxidase catalytic subunit have an ~50% reduction of complex IV activity in most tissues including muscle (7). This mouse manifests a higher percentage of ragged red muscle fibers; an altered mitochondrial morphology; and reduced ATP content in heart, spleen, liver, and skeletal muscle (7). Mice harboring the $ND5^{S204F}$ variant have not yet been described to show a mitochondrial phenotype, suggesting this mutation to be a nonpathogenic variant.

Nuclear mutations, for example, in the brain, heart, and muscle isoform 1 of the adenine nucleotide translocators (ANT1), have also been reported in patients with PMDs (8–10). The ANTs mediate the exchange of ATP and ADP from the mitochondria to the cytosol and vice versa. These mutations result in cardiac and skeletal muscle

Significance

Primary mitochondrial diseases (PMDs) are the most prevalent inborn metabolic disorders, affecting an estimated 1 in 4,200 individuals. Endurance exercise is generally known to improve mitochondrial function, but its indication in the heterogeneous group of PMDs is unclear. We determined the relationship between mitochondrial mutations, endurance exercise response, and the underlying molecular pathways in mice with distinct mitochondrial mutations. This revealed that mitochondria are crucial regulators of exercise capacity and exercise response. Endurance exercise proved to be mostly beneficial across the different mitochondrial mutant mice with the exception of a worsened dilated cardiomyopathy in ANT1-deficient mice. Thus, therapeutic exercises, especially in patients with PMDs, should take into account the physical and mitochondrial genetic status of the patient.

Author contributions: P.M.S. and D.C.W. designed research; P.M.S., A.B., W.T., and K.M. performed research; D.C.W. contributed new reagents/analytic tools; P.M.S. and K.R. analyzed data; and P.M.S. and D.C.W. wrote the paper.

Reviewers: B.G., AdventHealth Translational Research Institute; L.G., Joslin Diabetes Center; P.G.-R., Universitat de Barcelona; and D.C., University of California, Irvine.

Competing interest statement: D.C.W. is part of the scientific advisory boards for Pano Therapeutics and Medical Excellence Capital.

[1]To whom correspondence may be addressed. Email: wallaced1@email.chop.edu.

This article contains supporting information online at http://www.pnas.org/lookup/suppl/doi:10.1073/pnas.2200549119/-/DCSupplemental.

Published April 28, 2022.

myopathy with a massive proliferation of abnormal mitochondria (9, 10). Likewise, ANT1-deficient mice show ragged red muscle fibers, cardiomyopathy, and mitochondrial proliferation with minor uncoupling in both heart and skeletal muscle (11). On the molecular level, an induction of OxPhos enzymes both at the transcriptional and on the activity level was found in skeletal muscle (12, 13). Ant1 has been shown to regulate the mitochondrial permeability transition pore (14, 15), represent the primary proton channel for the mitochondrial inner membrane (16), and be essential for the function of PINK/Parkin mitophagy (17).

In addition to directly pathogenic mitochondrial mutations, region-specific mtDNA polymorphic lineages (haplogroups) (18, 19) have been associated with a broad spectrum of common diseases. These range from metabolic syndrome including diabetes, obesity, and cardiac and cardiovascular disease to neurological diseases including Alzheimer's and Parkinson's disease, cancer, and aging (1, 19).

Endurance exercise was shown to be beneficial in neurodegenerative and cardiovascular diseases by improving mitochondrial function (20, 21). However, whether or not exercise is indicated in PMDs is still unclear, with most patients displaying a strong exercise intolerance. Some studies suggest positive effects of moderate endurance exercise, improving exercise intolerance and quality of daily living (22–24). However, due to the heterogeneous nature of mitochondrial diseases, a general conclusion on the outcome of exercising is impossible without a deeper understanding of the molecular adaptions among the different mitochondrial mutations.

Endurance exercise disrupts the cellular homeostasis, resulting in a temporal energy depletion, increased ROS production, and alterations to the calcium levels and redox state (25, 26). These primary mediators activate downstream signaling pathways such as AMPK, calcineurin, or TNFα that mediate the adaptive response (27). In healthy subjects, this includes an increase in mitochondrial biogenesis and antioxidative capacity, up-regulation of glucose and lipid metabolism, and altered cell growth signaling (28).

Most of the primary molecular mediators of an exercise stimulus are directly associated with the mitochondria. The relationship between exercise and mitochondria is demonstrated by the enrichment of African mtDNA lineage L0 in long-distance runners versus enrichment of Eurasian J, Uk, and F in sprinters (29–35). Consequently, mitochondrial mutations in PMDs might affect not only the exercise capacity but also the exercise response.

Common exercise response pathways such as AMPK are often activated in patients with PMDs due to the continuous disruption of energy homeostasis (9). It follows, then, that additional activation of these pathways by exercise may benefit some PMD patients.

We hypothesize that the endurance exercise response and the physiological benefits vary strongly with the underlying mitochondrial mutations. To test this hypothesis, we have subjected a set of distinct mouse models of PMD to endurance exercise and investigated the effects on physiology and cellular and molecular parameters. These studies have revealed that different genetic defects have different responses to endurance exercise, suggesting that therapeutic exercises should take into account the physical and genetic status of the patient.

Results

To assess the effect of mitochondrial mutations on exercise capacity and response, we created mice harboring different mitochondrial mutations. These include C57BL/6 (B6) mice homoplasmic for mtDNA mutations in *ND6*^{P25L} or the *ND5*^{S204F} subunits of complex I, mice homoplasmic for the *CO1*^{V421A} mutation in a subunit of complex IV, and mice homozygous for the nDNA *Slc25a4*$^{-/-}$ (*ANT1*$^{-/-}$) mutation. We compared the exercise capacity and physiological as well as molecular response to an 8-wk endurance exercise protocol in 4- to 6-mo-old male mice.

Mitochondrial Mutant Mice Manifest Different Exercise Capacities. First, we assessed how the mtDNA and nDNA mitochondrial mutations affect exercise capacity. This was tested in 4- to 6-mo-old mice compared to B6 control mice.

The ND5^{S204F} baseline and exercise stress test. ND5 mice, compared to B6 controls, showed no differences in VO_2 (Fig. 1*A*) or respiratory exchange ratio (RER) (Fig. 1*B*) during rest but displayed reduced activity levels (Fig. 1*C*) and a trend toward a reduced voluntary running wheel activity (*SI Appendix*, Fig. S1*A*). However, in the exercise stress test, ND5 mice show tendencies toward improved VO_2max (Fig. 1*D*) and running time (Fig. 1*F*) but no changes in the RER during running (Fig. 1*E*). Among the ND5 mice, we found a positive correlation between VO_2max and running time (*SI Appendix*, Fig. S1*B*), similar to that seen among the B6 control mice, indicating a reliance on OxPhos during exercise.

Next, we assessed the two common limiting factors for VO_2max, which are heart function and muscle respiration. Using echocardiography, we found no impairment of left ventricular (LV) function or structure in ND5 mice relative to B6 controls (Fig. 2 *A* and *B* and *SI Appendix*, Fig. S2) and no correlation between ejection fraction and running time (*SI Appendix*, Fig. S2*E*), suggesting that heart function is not limiting exercise capacity. In skeletal muscle, high-resolution respirometry showed no deficiencies in mitochondrial respiration or ROS production in ND5 mice compared to control (Fig. 2 *C* and *D* and *SI Appendix*, Fig. S3), consistent with no changes in VO_2max and exercise capacity.

To screen for alterations in skeletal muscle function, we performed RNA sequencing (RNASeq) of the soleus muscle (Fig. 2*E*). We found a mild up-regulation of mitochondrial translation and the electron transport chain components in ND5 mice relative to B6 controls (*SI Appendix*, Fig. S4). To tease out the molecular determinants of the natural variability in the exercise capacity of ND5 mice, we correlated the RNASeq data of individual mice with their own individual exercise capacity data (*SI Appendix*, Fig. S5*A*). We found positive correlations of OxPhos and amino acid metabolism with running time (Fig. 2*G*), demonstrating that ND5 mice with a high expression of these genes exhibit a higher exercise capacity than littermates with a low expression of OxPhos and amino acid metabolism genes. Thus, these genes are determinants of the exercise capacity in ND5 mice. In contrast, we found no correlations of glycolytic gene expression or of beta oxidation with exercise capacity in ND5 mice (Fig. 2*G*). In summary, ND5 mice show no exercise intolerance, and their exercise capacity appears to be limited by the oxidative capacity of their skeletal muscle.

The ND6^{P25L} baseline and exercise stress test. ND6 mice, compared to B6 controls, showed no alterations in their basal metabolism (Fig. 1 *A* and *B*) except for reduced activity levels (Fig. 1*C*). In the exercise stress test, ND6 mice showed a consistent trend toward a lower VO_2max (Fig. 1*D*) and running time (Fig. 1*F*), indicating a mildly reduced exercise capacity. We did not detect any signs of an impaired heart function (Fig. 2 *A* and *B* and *SI Appendix*, Fig. S2), but ND6 mice displayed reduced mitochondrial respiration in skeletal muscle (Fig. 2*C*

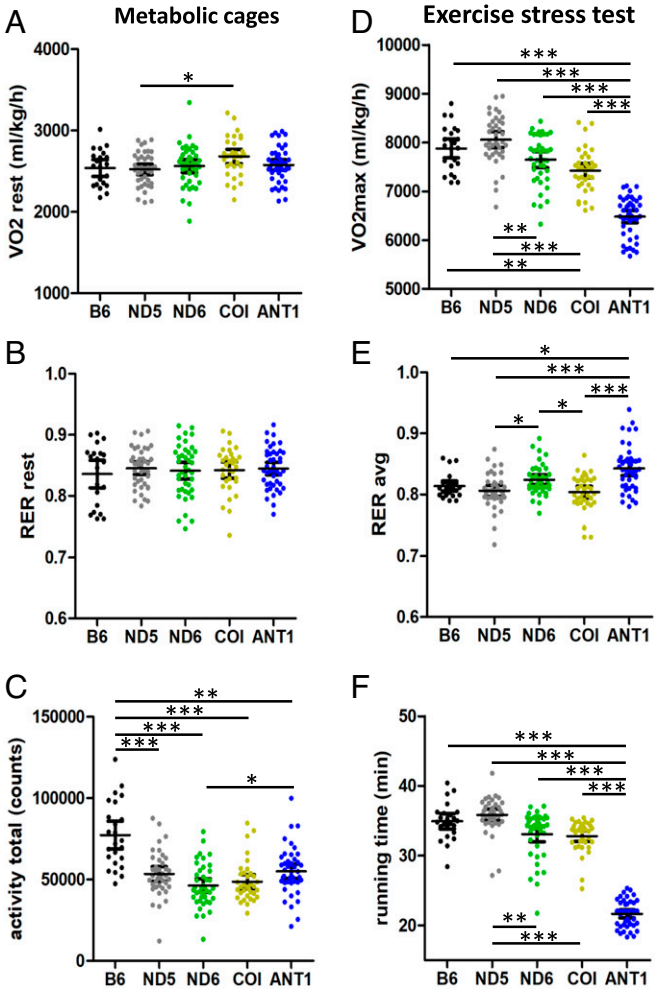

Fig. 1. Mitochondrial mutant mice mirror a range of mitochondrial disorders with varying severity. (*A* and *B*) Average oxygen uptake (VO_2) and RER (VCO_2/VO_2) of 4-mo-old mice while resting in the CLAMS. (*C*) Total activity count of 4-mo-old mice during 24 h in the CLAMS. (*D*) Maximal oxygen uptake and (*E*) average RER during an exercise stress test ramp-up protocol in 4-mo-old mice. (*F*) Time until 4-mo-old mice fulfill the exhaustion criteria in the exercise stress test ramp-up protocol. Each data point represents one mouse (n = 21 to 44) with bars indicating median and 95% confidence intervals for all graphs. Significances between strains were tested using one-way ANOVA and are indicated by asterisks (*P < 0.05, **P < 0.01, ***P < 0.0001).

and *SI Appendix*, Fig. S3). RNASeq of skeletal muscle demonstrated a moderate up-regulation of mitochondrial gene expression (*SI Appendix*, Fig. S4), consistent with a trend toward an increase in mitochondrial mass (*SI Appendix*, Fig. S3*E*). We again correlated gene expression with exercise capacity on the individual mouse level. This revealed positive correlations for OxPhos, amino acid metabolism, and beta oxidation (Fig. 2*G*), indicating oxidative metabolism is an important determinant of exercise capacity in ND6 mice. In summary, ND6 mice show a mild exercise intolerance due to a reduced mitochondrial respiratory capacity of skeletal muscle.

The* COI^{V421A} *baseline and exercise stress test. CO1 mice, relative to B6 controls, showed reduced general activity levels (Fig. 1*C*), a decreased VO_2max (Fig. 1*D*), and a trend toward a decreased running time (Fig. 1*F*) during the exercise stress test. Interestingly, in analyzing the individual COI mice, we found no correlation between VO_2max and running time (*SI Appendix*, Fig. S1*B*), indicating a lower reliance on oxidative metabolism during exercise. However, this is in contrast to a strong positive correlation between OxPhos gene expression and exercise capacity (again on the individual mouse level) in the CO1 skeletal muscle (Fig. 2*G*). Compared to B6 controls, skeletal muscle respiration tends to be lower across all respiratory states, although not reaching significance (Fig. 2*C* and *SI Appendix*, Fig. S3). Consistent with a compensatory up-regulation of mitochondrial biogenesis, we found a trend toward an increased mitochondrial mass (*SI Appendix*, Fig. S3*E*) and increased OxPhos gene expression (*SI Appendix*, Fig. S4). Heart function was not negatively affected in CO1 mice (Fig. 2 *A* and *B* and *SI Appendix*, Fig. S2). In summary, CO1 mice show a moderate exercise intolerance, partially due to a decreased mitochondrial respiration.

The Ant1*$^{-/-}$ *baseline and exercise stress test. ANT1 mice, compared to B6 controls, showed a drastically reduced VO_2max (Fig. 1*D*) and running time (Fig. 1*F*) in the exercise stress test. Consistent with previous reports (11), ANT1 mice displayed a compensated cardiomyopathy with reduced ejection fraction (Fig. 2*A*), thickening of the LV posterior wall (LVPW) (*SI Appendix*, Fig. S2*A*), and increased LV mass (Fig. 2*B*) but unaltered stroke volume (*SI Appendix*, Fig. S2*D*). In skeletal muscle, mitochondrial respiration normalized to mitochondrial mass is strongly reduced (Fig. 2*C* and *SI Appendix*, Fig. S3 *A* and *B*), while ROS production is increased (Fig. 2*D*). Mitochondrial mass in skeletal muscle is increased (*SI Appendix*, Fig. S3*E*), consistent with a strong induction of mitochondrial gene expression (*SI Appendix*, Fig. S4). When looking at individual ANT1 mice, VO_2max is not correlated to running time (*SI Appendix*, Fig. S1*B*). This is confirmed by a strong negative correlation of OxPhos gene expression with running time in skeletal muscle (Fig. 2*G*). Thus, the exercise capacity of ANT1 mice does not rely on OxPhos, which is consistent with impaired mitochondrial ATP export to the cytosol. Individual ANT1 mice with a higher OxPhos gene expression have a lower exercise capacity (Fig. 2*G*). This could be a result of the most severely affected ANT1 mice having the highest compensatory induction of mitochondrial biogenesis, or it could be that more mitochondria deplete the muscle fibers of substrates for glycolysis. Consistent with impaired OxPhos, we found evidence of an increased carbohydrate metabolism during exercise due to an increased RER during running (Fig. 1*E*), although we found no correlation between expression of glycolytic genes in skeletal muscle and running time among the ANT1 mice (Fig. 2*G*).

ANT1 mice not only display a very distinct gene expression profile in skeletal muscle (Fig. 2*E*), the molecular determinants of exercise capacity are also strongly altered. Forty-one of 54 pathways that correlate with a high running time in the ANT1 mice are negatively correlated with running time in the B6 mice (Fig. 2*F*). Vice versa, out of the 46 pathways that correlate positively with running time in the B6 mice, none correlate positively in the ANT1 mice, and 13 are even associated with a low running time (Fig. 2*F*). In summary, ANT1 mice display a severe exercise intolerance with underlying cardiac and skeletal muscle pathology and strongly altered determinants of exercise capacity. This implies that activation of no single pathway would likely increase the exercise capacity of both B6 mice and ANT1 mice, highlighting the potential importance of differential exercise recommendations for different PMDs.

The differential exercise capacity of mitochondrial mutations. Distinct mitochondrial mutations affect exercise capacity differently, resulting in no (ND5) to severe (ANT1) exercise intolerance (Table 1). In addition, by correlating skeletal muscle gene expression to running time, we identified four crucial molecular determinants of exercise capacity: oxidative phosphorylation, the extracellular matrix (ECM) matrisome, amino acid metabolism, and cell cycle regulation. While there is a well-known connection

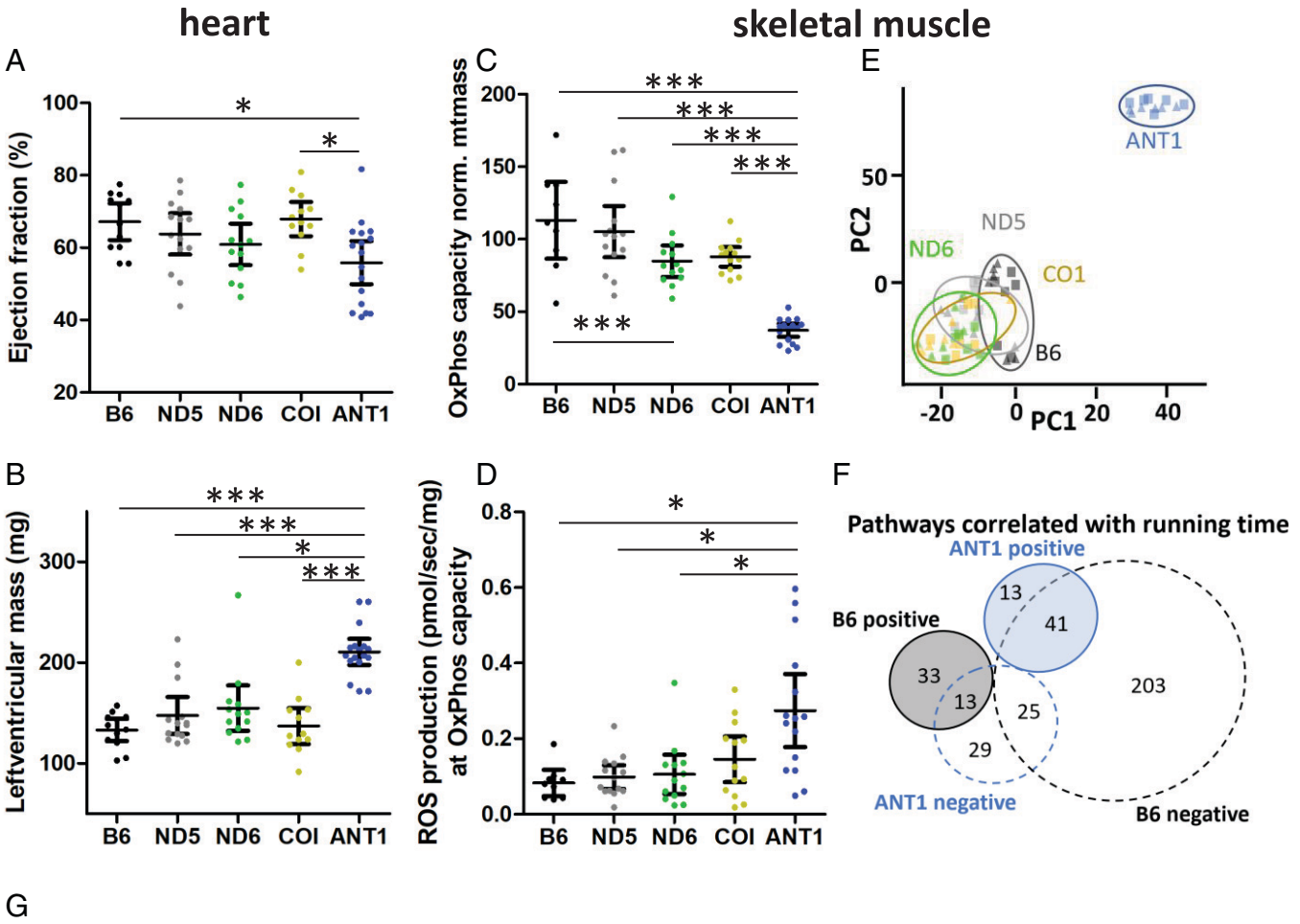

G

Pathways correlated with running time	B6	ND5	ND6	COI	ANT1
Hallmark Oxidative Phosphorylation	5.89E-35	1.24E-04	2.26E-22	1.40E-08	9.66E-13
Reactome Mitochondrial Fatty Acid Beta Oxidation	5.90E-08	3.40E-01	2.00E-02	2.00E-02	2.00E-02
Hallmark Glycolysis	2.00E-01	6.00E-01	3.40E-01	7.70E-01	7.60E-01
Reactome Metabolism of Amino Acids	4.85E-06	3.25E-14	1.23E-04	6.65E-04	2.53E-16
Hallmark ROS Pathway	3.30E-01	2.17E-03	2.00E-01	3.50E-01	6.50E-01

Fig. 2. Mitochondrial mutations alter determinants of exercise capacity. (*A*) Ejection fraction and (*B*) LV mass of hearts of 6-mo-old, nonexercised mice measured by echocardiography. (*C*) Coupled respiration in the presence of complex I and II substrates (OxPhos capacity) normalized to mitochondrial mass in soleus muscle of 6-mo-old, nonexercised mice. (*D*) ROS production at OxPhos capacity normalized to tissue mass in soleus muscle of 6-mo-old, nonexercised mice. Each data point represents one mouse (n = 9 to 17) with bars indicating median and 95% confidence intervals for all graphs. Significances between strains were tested using one-way ANOVA and are indicated by asterisks (*P < 0.05, **P < 0.01, ***P < 0.0001). (*E–G*) RNASeq of soleus muscle in 6-mo-old mice (n = 6 per strain for each exercise-trained and nonexercised). t-distributed stochastic neighbor embedding (t-SNE) clustering of the expression profile (*E*) of exercised (triangle) and nonexercised (square) mice. Venn diagram (*F*) displaying the overlap of pathways that correlate positively (filled circles) or negatively (dashed circles) with running time in the exercise stress test in ANT1 (blue) or B6 control mice (black). (*G*) Correlation of energy metabolism gene sets with running time in the exercise stress test within each mouse strain. *P* values are indicated in the table and visualized by color richness, and directionality of the correlation is indicated by color (blue, positive correlation; red, negative correlation).

between expression of OxPhos genes and, perhaps, amino acid metabolism and exercise capacity, much less is known about the role of the expression of ECM genes and the regulation of p27 and p21 in shaping exercise capacity. Notably however, none of the four determinants correlate in the same direction in all five mouse strains (*SI Appendix*, Fig. S5*B*), demonstrating how different mitochondrial mutations affect determinants of exercise capacity in different ways.

Mitochondrial Mutations Alter the Responsiveness to Endurance Exercise. To determine if endurance exercise is beneficial for the different mitochondrial mutant mice, 4-mo-old mice of the five genetic strains were subjected to an 8-wk endurance exercise regimen in which the mice ran every second day for 45 min at 50% of the maximal speed reached in the initial exercise stress test. We tested the exercise performance using both the exercise stress test and the calorimetry before (Fig. 1 and *SI Appendix*, Fig. S1) and after the 8-wk exercise regimen (Fig. 3; *SI Appendix*, Fig. S6; and Dataset S12). The exercise trained group of mice were compared to a control group of genotype and age matched untrained (rested) mice using the following formula: (exercise trained $_{post}$/exercise trained $_{prior}$)/(untrained [rested] $_{post}$/untrained [rested] $_{prior}$). Thus, deviation from 1 indicates the effects of training relative to untrained controls.

Effects of exercise training on B6 mice. In B6 mice, exercise training did not significantly alter VO_2 or RER at rest (Fig. 3 *A* and *B*) However, it resulted in significant improvement in

Table 1. Overview of physiology of nonexercised mitochondrial mutant mice compared to control mice

Nonexercised compared to B6 control	ND5	ND6	COI	ANT1
CLAMS				
VO_2 rest (Fig. 1*A*)	n.s.	n.s.	n.s.	n.s.
RER rest (Fig. 1*B*)	n.s.	n.s.	n.s.	n.s.
Activity (Fig. 1*C*)	***	***	***	**
Running wheel (*SI Appendix*, Fig. S1*A*)	n.s.	n.s.	n.s.	n.s.
Weight (*SI Appendix*, Fig. S1*C*)	n.s.	n.s.	n.s.	n.s.
Heat production (*SI Appendix*, Fig. S1*D*)	n.s.	n.s.	n.s.	n.s.
Exercise stress test				
VO_2max (Fig. 1*D*)	n.s.	n.s.	**	***
RER average (Fig. 1*E*)	n.s.	n.s.	n.s.	*
Running time (Fig. 1*F*)	n.s.	n.s.	n.s.	***
Skeletal muscle respirometry				
OxPhos capacity (Fig. 2*C*)	n.s.	***	n.s.	***
ROS production at OxPhos (Fig. 2*D*)	n.s.	n.s.	n.s.	*
ETS capacity (*SI Appendix*, Fig. S3*A*)	n.s.	**	n.s.	***
Complex I capacity (*SI Appendix*, Fig. S3*B*)	n.s.	n.s.	n.s.	***
Leak/ETS (*SI Appendix*, Fig. S3*C*)	n.s.	n.s.	n.s.	n.s.
Mitochondrial mass (*SI Appendix*, Fig. S3*D*)	n.s.	n.s.	n.s.	***
Echocardiography				
Ejection fraction (Fig. 2*A*)	n.s.	n.s.	n.s.	*
LV mass (Fig. 2*B*)	n.s.	n.s.	n.s.	***
LVPW,d (*SI Appendix*, Fig. S2*A*)	n.s.	n.s.	n.s.	*
LVAW,d (*SI Appendix*, Fig. S2*B*)	n.s.	n.s.	n.s.	n.s.
Diameter diastole (*SI Appendix*, Fig. S2*C*)	n.s.	n.s.	n.s.	n.s.
Stroke volume (*SI Appendix*, Fig. S2*D*)	n.s.	n.s.	n.s.	n.s.

Physiology of nonexercised mitochondrial mutant mice compared to nonexercised control mice. Color indicates directionality (red indicates down, blue indicates up, and white indicates no difference), and color richness indicates strength of effect. Significances are indicated by stars (*$P < 0.05$, **$P < 0.01$, ***$P < 0.0001$).

VO_2max and running time in the subsequent exercise stress test (Fig. 3 *C* and *D*) but without altering RER during running (Fig. 3*E*). Exercise training reduced body weight (*SI Appendix*, Fig. S6*A*) and increased voluntary running wheel activity (*SI Appendix*, Fig. S6*B*) but had no significant effect on activity levels (*SI Appendix*, Fig. S6*C*). Thus, B6 control mice show a beneficial, physiological response to exercise training (Fig. 3*F*, dark gray). We did not find alterations in heart function (Fig.4 *A–C* and *SI Appendix*, Fig. S7 *A–C*) or skeletal muscle respiration (Fig.4 *E–G* and *SI Appendix*, Fig. S7 *D–G*) in B6 mice upon exercise training, suggesting that the improved exercise capacity is mediated by increased oxygen availability to the muscles. To identify pathways mediating the response to exercise training, we compared the gene expression profiles of soleus muscle between exercise-trained and nonexercised B6 mice. Surprisingly, we found no major differences in gene expression except for a modest up-regulation of type II interferon signaling (*SI Appendix*, Fig. S8), indicating a mild immune system activation upon exercise training.

Next, we correlated gene expression with the improvement in running time among the individual exercise-trained B6 mice (*SI Appendix*, Fig. S9*A*). This correlation allowed us to identify pathways that are either mediators or determinants of exercise response; if genes are significantly correlated and differentially expressed between trained and untrained mice, these genes would be considered a mediator with the causality being as follows: training → gene expression → running time. If genes are significantly correlated and not differentially expressed as a result of training, they are static determinants of exercise response; i.e., the genes may affect exercise response, but the training does not change the expression of the genes.

Specifically, at the individual mouse level we found a positive correlation between OxPhos gene expression and improvement in running time with training (*SI Appendix*, Fig. S9*B*). However, analysis of trained vs. untrained mice showed that OxPhos gene expression was not up-regulated upon exercise training in B6 mice; rather, mice that had higher Oxphos gene expression pretraining responded better to training, while mice with lower initial Oxphos gene expression did not improve as significantly. This indicates that OxPhos gene expression is a determinant for exercise response, rather than a mediator. In summary, B6 control mice respond positively to exercise training, which is most likely due to systemic adaptions (e.g., increase in oxygen transport to the muscle) since no increase in skeletal muscle oxidative capacity was seen as a result of training.

Effects of exercise training on* ND5^{S204F} *mice. Contrary to B6 mice, ND5 mice showed no improvement in either VO_2max or running time upon exercise training (Fig. 3 *C* and *D*). Exercise training even decreased OxPhos capacity (Fig. 4*E*) and CI capacity (*SI Appendix*, Fig. S7*E*) in skeletal muscle of ND5 mice. This is partially compensated by a trend toward a higher mitochondrial mass (*SI Appendix*, Fig. S7*F*) and an induction of OxPhos gene expression in skeletal muscle (*SI Appendix*, Fig. S8). ND5 mice further showed an induction of stress response genes (*SI Appendix*, Fig. S8) upon exercise training, but ROS levels in skeletal muscle were not altered (Fig. 4*F*). Similarly, heart function was not compromised in exercise-trained ND5 mice (Fig. 4 *A–C*). In summary, ND5 mice demonstrate the strongest transcriptional response in skeletal muscle upon exercise training but did not improve with respect to their exercise capacity and muscle oxidative capacity, possibly due to activation of the stress response.

Effects of exercise training on* ND6^{P25L} *mice. ND6 mice improved upon exercise training with respect to both VO_2max (Fig. 3*C*) and running time (Fig. 3*D*), but activity levels were slightly lowered (*SI Appendix*, Fig. S6*C*), consistent with a minor decrease in heat production (*SI Appendix*, Fig. S6*D*). Voluntary running wheel activity was not negatively affected in exercise-trained ND6 mice (*SI Appendix*, Fig. S6*B*). In addition, the ND6 mice showed a reduced RER during running (Fig. 3*E*), indicating an increased beta-oxidation. In skeletal muscle, we detected an increased complex I respiration (*SI Appendix*, Fig. S7*E*) and a trend toward an increased OxPhos capacity (Fig. 4*E*), suggesting that the improvement in exercise physiology is due to an improved skeletal muscle oxidative capacity. However, we found a slight increase in mitochondrial mass (*SI Appendix*, Fig. S7*G*) but no induction of mitochondrial gene expression (*SI Appendix*, Fig. S8) in ND6 mice upon exercise training. Heart function was not altered (Fig. 4 *A–C*). In summary, ND6 mice respond well to exercise training, improving in their exercise capacity due to increased muscle oxidative capacities.

Effects of exercise training on* COI^{V421A} *mice. CO1 mice improved in their VO_2max (Fig. 3*C*) but not their running time (Fig. 3*D*) upon exercise training. The improvement in one but not the other parameter is in line with the absence of a correlation between both parameters that we already observed when we compared the individual CO1 mice prior to exercise training (*SI Appendix*, Fig. S1*B*). Similar to ND6 mice, exercise-trained CO1 mice display reduced activity levels (*SI*

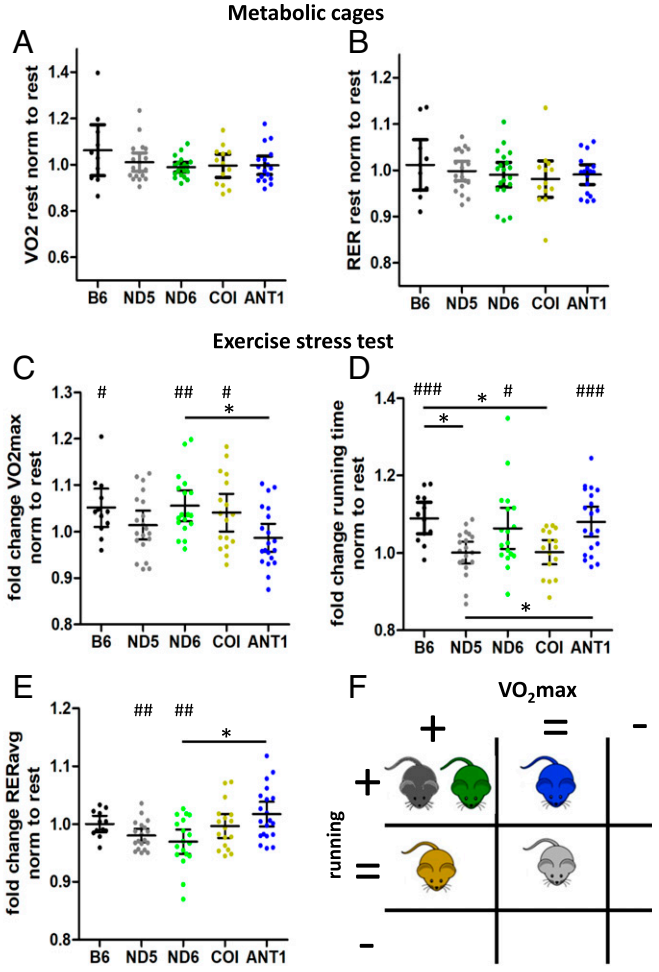

Fig. 3. Mitochondrial mutations modify physiologic exercise response. Fold change in (*A*) VO_2 and (*B*) RER while resting in the CLAMS upon exercise training in 6-mo-old mice, normalized to age-matched, nonexercised littermates. Fold change in (*C*) VO_2max, (*D*) running time, and (*E*) average RER in the exercise stress test upon exercise training in 6-mo-old mice, normalized to age-matched, nonexercised littermates. Each data point represents one mouse (n = 12 to 22) with bars indicating median and 95% confidence intervals for all graphs. Significances between strains were tested using one-way ANOVA and are indicated by asterisks, and significances between exercised and nonexercised were tested using t test and are indicated by # (*$P < 0.05$, $^{\#}P < 0.05$, $^{\#\#}P < 0.01$, $^{\#\#\#}P < 0.0001$). (*F*) Scheme visualizing the response to exercise training. B6 control (dark gray) and ND6 (green) improve (+) in VO_2max and running time. ANT1 (blue) and CO1 (yellow) mice only improve in one but not the other parameter, whereas ND5 mice (light gray) do not improve (=) at all.

Appendix, Fig. S6*C*) and a lower weight gain (*SI Appendix*, Fig. S6*A*) but no other alterations in their basal metabolism (Fig. 3 *A* and *B* and *SI Appendix*, Fig. S6). In skeletal muscle, we found trends toward an increased electron transport system (ETS) capacity and complex I (CI) respiration (*SI Appendix*, Fig. S7 *D* and *E*) and reduced ROS production (Fig. 4*F*). These changes, in combination with possible systemic adaptions, could account for the increased VO_2max. We detected no consistent transcriptional response except for an up-regulation of a few glycolytic genes (*SI Appendix*, Fig. S8) in skeletal muscle and no changes to heart function (Fig.4 *A*–*C*) in CO1 mice upon exercise training. In summary, CO1 mice demonstrate a small but beneficial response to exercise training.

Effects of exercise training on* Ant1$^{-/-}$ *mice. ANT1 mice improved in their running time (Fig. 3*D*) but not their VO_2max (Fig. 3*C*) with exercise training. In skeletal muscle, we found an increased ETS capacity (*SI Appendix*, Fig. S7*D*) but no alterations in OxPhos capacity (Fig. 4*E*) or mitochondrial mass (*SI Appendix*, Fig. S7 *F* and *G*), which explains the unaltered VO_2max. However, we observed a significantly reduced leak/ETS capacity respiratory control ratio (Fig. 4*G*) and a lower ROS production (Fig. 4*F*), suggesting that exercise training may have stimulated the removal of damaged mitochondria, which had accumulated due to inhibition of mitophagy in the unexercised ANT1-deficient mice. We observed a higher RER during running (Fig. 3*E*), suggesting increased carbohydrate utilization, but did not find transcriptional alterations in skeletal muscle glycolytic genes (*SI Appendix*, Fig. S8). Exercise training worsened the LV function in ANT1 mice associated with significantly reduced ejection fraction (Fig. 4*A*), an increased LV diameter during diastole (Fig. 4*B*), and an increased LV mass (Fig. 4*C*) but without changes to LV wall thickness (*SI Appendix*, Fig. S7*A* and *B*). Stroke volume was not affected (*SI Appendix*, Fig. S7*C*), which explains why the worsened dilated cardiomyopathy in exercise-trained ANT1 mice did not impact exercise capacity.

To understand the molecular mechanisms that underlie the cardiomyopathy and its exercise-induced aggravation in ANT1 mice, we performed RNASeq of the heart in six exercise-trained and six nonexercised mice. First, we correlated the gene expression to ejection fraction among all individuals of the ANT1 strain, identifying pathways that are associated with a low cardiac function among the ANT1 mice (*SI Appendix*, Fig. S10, and Fig. 4*D*, second column). Then we identified pathways that are altered in ANT1 hearts upon exercise training (*SI Appendix*, Fig. S10, and Fig. 4*D*, third column). Combining both approaches revealed eight candidate pathways that could mediate the worsening of the dilated cardiomyopathy in ANT1 mice, spanning cellular stress response, amino acid metabolism, translation, immune activation, and signal transduction (Fig. 4*D*). For example, high expression levels of the amino acid metabolism are associated with a low ejection fraction in ANT1 mice, and amino acid metabolism is up-regulated in ANT1 hearts upon exercise training. In summary, exercise training improved exercise capacity in ANT1 mice, perhaps by removing damaged mitochondria and by increasing the efficiency of the ETS in the muscle. However, exercise training aggravated the mild, preexisting cardiomyopathy in ANT1 mice, possibly by inducing the cellular stress response or altering the amino acid metabolism, constituting the first negative effect of exercise training in any of the mitochondrial mutant mice.

Differential effects of exercise training on mitochondrial mutations. To sum up, mitochondrial mutations can alter the exercise response dramatically, resulting in high responders (B6 control and ND6 mice), partial/low responders (ANT1 and CO1 mice), and nonresponders (ND5 mice) (Fig. 3*F*) with the latter one being the most surprising given how little of an effect the ND5 mutation had on baseline (untrained) exercise capacity (Fig. 1 *D* and *F*). To evaluate if the chosen exercise training intensity affected the exercise response, we correlated the average number of shocks each mouse received during the training period (surrogate marker for individual exercise training intensity) with their exercise response. We did not find any significant correlations for either VO_2max (*SI Appendix*, Fig. S11*A*) or running time (*SI Appendix*, Fig. S11*B*) with the exercise training intensity in any of the strains, providing no evidence for a suboptimal training intensity.

On the gene expression level, mitochondrial mutations altered the determinants of exercise response (*SI Appendix*, Fig. S9*B*), consistent with the observed alterations in exercise

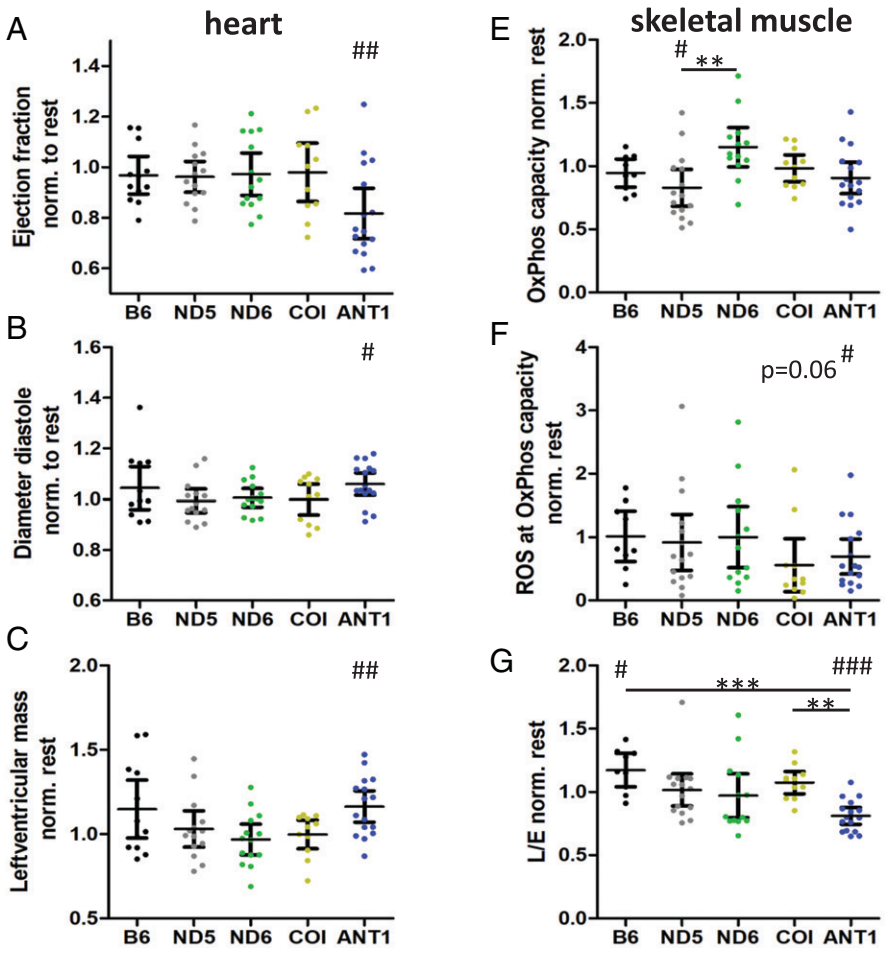

D Pathways correlated to EF and altered upon exercise in ANT1 mice

pathway	adj p-value correlation	p-value exercise
REACTOME_CELLULAR_RESPONSES_TO_EXTERNAL_STIMULI	9.83E-06	4.00E-02
REACTOME_SIGNALING_BY_ROBO_RECEPTORS	2.99E-04	2.80E-02
REACTOME_METABOLISM_OF_AMINO_ACIDS_AND_DERIVATIVES	3.43E-04	0.00E+00
REACTOME_METABOLISM_OF_RNA	1.03E-03	3.00E-02
REACTOME_RRNA_PROCESSING	3.27E-03	1.20E-02
REACTOME_INFLUENZA_INFECTION	5.08E-03	1.60E-02
REACTOME_SELENOAMINO_ACID_METABOLISM	2.30E-02	1.80E-02
REACTOME_GAP_JUNCTION_TRAFFICKING_AND_REGULATION	2.90E-02	3.80E-02

Fig. 4. Mitochondrial mutations alter the exercise response of heart and skeletal muscle. Fold change in (*A*) ejection fraction, (*B*) diastolic LV diameter, and (*C*) LV mass in hearts of exercise-trained mice normalized to nonexercised littermates (n = 12 to 17). (*D*) RNA-Seq of the heart (n = 6 per strain for both exercised and nonexercised). Gene sets that correlate significantly with ejection fraction in ANT1 mice (*P* values in column 2), and are altered in the opposite direction in exercised versus rested ANT1 mice (*P* values in column 3), represent candidate pathways to mediate the dilated cardiomyopathy in exercise-trained ANT1 mice. Fold change in (*E*) OxPhos capacity, (*F*) ROS production, and (*G*) leak respiration/ETS capacity respiratory control ratio (L/E) in soleus muscle of exercise-trained mice normalized to nonexercised littermates. Each data point represents one mouse (n = 9 to 16) with bars indicating median and 95% confidence intervals for all graphs. Significances between strains were tested using one-way ANOVA and are indicated by asterisks, and significances between exercised and nonexercised were tested using t test and are indicated by # ($^{\#}P < 0.05$, $^{**}P < 0.01$, $^{\#\#}P < 0.01$, $^{***}P < 0.0001$, $^{\#\#\#}P < 0.0001$).

capacity (*SI Appendix*, Fig. S5*B*). We revealed a total of 19 pathways that reached significance in all five strains, encompassing OxPhos, amino acid metabolism, the matrisome, and translation (*SI Appendix*, Fig. S9*B*). Out of these 19 pathways, only expression of OxPhos and TCA cycle genes showed a uniform directionality across all five mouse strains (*SI Appendix*, Fig. S9*B*), suggesting these pathways could serve as predictive markers for endurance exercise response. Last, we asked if the expression of any individual gene could act as a predictive marker of exercise response. However, no single gene showed a significant correlation with exercise response and uniform directionality of the correlation in more than three mouse strains (*SI Appendix*, Fig. S9*C*). Thus, our results demonstrate that the various mitochondrial mutations have differing effects on exercise physiology, resulting not only in an altered exercise response but also in modification of cellular and molecular determinants of exercise capacity and response (Table 2). While endurance exercise proved mostly beneficial in mitochondrial mutant mice, the aggravation of cardiomyopathy in one out of five strains warns against a generalized exercise recommendation in PMD patients and emphasizes the need to take into account their specific mutations.

Discussion

Analyzing the effects of endurance exercise on our mouse models with defined but distinct mitochondrial mutations has produced three important findings. First, we demonstrated the crucial role of mitochondria in mediating and shaping the exercise response. This is true not only for severe mitochondrial mutations such as the ND6, COI, and ANT1 that heavily impact the exercise capacity but also for the mild ND5 variant which abrogated endurance exercise response despite no effect on the general exercise capacity at baseline. Second, we showed that mitochondrial mutations can modify the exercise physiology profoundly, thereby changing determinants of exercise capacity. While generally, activation of mitochondrial biogenesis is considered a key factor in the positive adaption to endurance exercise, we revealed that it correlates with a low exercise capacity in some mitochondrial mutant mice. Consequently,

Table 2. Overview of effects of exercise training on mitochondrial mutant mice

Exercised compared to nonexercised	B6	ND5	ND6	COI	ANT1
CLAMS					
VO_2 rest (Fig. 3*A*)	n.s.	n.s.	n.s.	n.s.	n.s.
RER rest (Fig. 3*B*)	n.s.	n.s.	n.s.	n.s.	n.s.
Weight (*SI Appendix*, Fig. S5*A*)	#	##	#	#	#
Running wheel (*SI Appendix*, Fig. S5*B*)	#	n.s.	n.s.	n.s.	n.s.
Activity (*SI Appendix*, Fig. S5*C*)	n.s.	n.s.	#	###	#
Heat production (*SI Appendix*, Fig. S5*D*)	n.s.	n.s.	#	n.s.	n.s.
Exercise stress test					
VO_2max (Fig. 3*C*)	#	n.s.	##	#	n.s.
Running time (Fig. 3*D*)	###	n.s.	#	n.s.	###
RER average (Fig. 3*E*)	n.s.	##	##	n.s.	n.s.
Skeletal muscle respirometry					
OxPhos capacity (Fig. 4*E*)	n.s.	#	n.s.	n.s.	n.s.
ROS production at OxPhos (Fig. 4*F*)	n.s.	n.s.	n.s.	n.s.	#
Leak/ETS (Fig. 4*G*)	#	n.s.	n.s.	n.s.	###
ETS capacity (*SI Appendix*, Fig. S6*D*)	##	n.s.	n.s.	n.s.	#
Complex I capacity (*SI Appendix*, Fig. S6*E*)	#	##	#	n.s.	n.s.
Mitochondrial mass (*SI Appendix*, Fig. S6*F*)	n.s.	n.s.	##	n.s.	n.s.
Echocardiography					
Ejection fraction (Fig. 4*A*)	n.s.	n.s.	n.s.	n.s.	##
Diameter diastole (Fig. 4*B*)	n.s.	n.s.	n.s.	n.s.	#
LV mass (Fig. 4*C*)	n.s.	n.s.	n.s.	n.s.	##
LVPW,d (*SI Appendix*, Fig. S6*A*)	n.s.	n.s.	#	n.s.	n.s.
LVAW,d (*SI Appendix*, Fig. S6*B*)	n.s.	n.s.	n.s.	n.s.	n.s.
Stroke volume (*SI Appendix*, Fig. S6*C*)	n.s.	n.s.	n.s.	n.s.	n.s.

Physiology of exercise-trained mitochondrial mutant mice compared to nonexercised control mice. Color indicates directionality (red indicates down, blue indicates up, and white indicates no difference), and color richness indicates strength of effect. Significances are indicated by pound symbols ($^{\#}P < 0.05$, $^{\#\#}P < 0.01$, $^{\#\#\#}P < 0.0001$).

different mitochondrial mutations change not only the pathways activated by endurance exercise but also the physiologic consequences of their activation. By correlating skeletal muscle and heart expression profiles with physiologic readouts of the same mice, we provide a valuable resource that allows us to decipher the effect of mitochondria on molecular mediators of exercise. Last, our study provides evidence that endurance exercise generally has the potential to benefit patients with PMDs, though caution is warranted; the exact benefits of endurance exercise vary depending on the underlying mutation, and although some positive adaptations seem to occur in all tested strains, in the case of the ANT1 mutant, these positive adaptations are negated by the increased severity of the existing cardiomyopathy.

It is well known that there is a high variability in the adaptive response to exercise, which in rare cases can even be adverse (36). This variability originates from differences in age, gender, genotype, nutritional status, exercise modality, and homeostatic stress conferred by the exercise stimulus (37). A genome-wide association study found 21 single nucleotide polymorphisms (SNPs) that account for half of the trainability in VO_2max, with an SNP in an enzyme involved in lipid metabolism being the most prominent (38). Similarly, SNPs in genes regulating electrolyte balance (39), ROS (40), skeletal muscle differentiation (41), and oxygen delivery (42, 43) were associated with an altered exercise capacity and response. The Heritage Family Study estimated a heritability of ∼50% for the VO_2max increase upon a standardized exercise protocol. This human study suggested that a predominantly maternally inherited factor mediated VO_2max response to exercise with the paternal effect being environmental rather than genetic (44). This is consistent with the mtDNA playing an important role in shaping exercise response and previous studies reporting correlations between mtDNA polymorphisms and exercise capacity and trainability (45, 46).

Different mitochondrial mutations resulted in distinct physiologic and cellular adaptions to endurance exercise training. B6 control mice improved in VO_2max and running time but did not show improved skeletal muscle respiration, indicating a central limitation and improved oxygen delivery to the muscles. Similarly, ND6 mice improved in VO_2max and running time, which could be attributed to improved muscle respiration upon exercise training. In contrast, ANT1 mice showed an improvement in running time but not VO_2max, likely mediated by an increased glycolytic flux and increased OxPhos efficiency. Last, ND5 mice demonstrated no improvement in exercise capacity and even decreased mitochondrial respiration upon exercise training, which is consistent with a recent study reporting that a person harboring an ND5 variant had increased exercise capacity but abrogated exercise response (45). Taken together, our results emphasize the strong effect of mitochondrial variants and mutations on the adaptive response to exercise training.

Recent progress in multiomics has primed further interest in understanding the molecular transducers of exercise (47) and the identification of biomarkers for exercise capacity and response (48). In line with this idea, we correlated the expression profile of skeletal muscle with the exercise capacity of the individual mitochondrial mutant mice. This revealed key determinants of exercise capacity and response. These include expected candidates such as genes involved in OxPhos, amino acid metabolism, or lipid metabolism but also less expected pathways such as the matrisome. It is known that the ECM plays an important role in tissue responses to injury (49) and that exercise stimulates collagen synthesis and ECM turnover rate (50). Here we demonstrate that ECM gene expression is a determinant of both exercise capacity and response in mice, which confirms previous evidence (51).

Even more importantly, we revealed that the pathways associated with a high exercise capacity or beneficial exercise response are different between the mitochondrial mutant mouse models. Interestingly, the importance of certain pathways as determinants of exercise capacity and response did not only shift between mitochondrial mutant mouse models but even switched directionality. For example, control mice with a high expression of OxPhos genes perform better in an exercise stress test than littermates with a lower expression of OxPhos genes. In contrast, in ANT1 mice, those with a low expression of OxPhos genes perform better in the exercise stress test. This counterintuitive observation is likely due to ANT1 mice mostly relying on glycolytic metabolism for energy production during exercise.

For the matrisome, it would be expected that a high expression and thus high ECM turnover correlate with a positive exercise

response. While this is true in ANT1 mice, CO1 mice show a strong negative correlation of ECM expression with the physiologic exercise response. ECM homeostasis is a balance between anabolic and catabolic processes, and it was shown that metabolic disorders can result in a dysbalance (52). Thus, our results point to the ECM homeostasis being affected differently in ANT1 and CO1 mice, thereby explaining the opposite directionality of the correlation of matrisome gene expression with exercise capacity in those strains and pointing to a role for mitochondria in ECM regulation and connective tissue disorder.

Taken together, mitochondrial mutations affect both the exercise response as well as its determinants. This implies that there may not be universal biomarkers for exercise response, since a marker that correlates with a beneficial exercise response in individuals of one mitochondrial genotype might correlate with an adverse exercise response in individuals of another mitochondrial genotype. Indeed, this finding might explain the relatively small overlap of predictors of exercise capacity identified in different studies (53) and emphasizes the need to account for the mitochondrial genotype in future trials.

Our findings have particular significance for mitochondrial patients, highlighting the need for personalized prescriptions of physical activity dependent on the underlying mitochondrial mutation. The same is true for the use of exercise mimetics, given the significant changes in determinants of exercise capacity with the different mitochondrial mutations. Unfortunately, we could not identify reliable predictors for exercise capacity that are valid across all mitochondrial mutant mice. In contrast, high expression of OxPhos genes was correlated with a high physiologic exercise response across all strains. Given that we did not observe an up-regulation of OxPhos genes with exercise, this indicates that the expression levels of OxPhos genes could serve as a predictor for exercise response.

Some limitations of our study are important to consider. First, we only used male mice since males are often more affected by mitochondrial disorders. However, sex might be a crucial biological variable that future studies would need to address to allow generalizable conclusions. Second, we focused mostly on parameters associated to a peripheral limitation (oxygen consumption by skeletal muscle) instead of central limitation (oxygen transport to the muscle) since a peripheral limitation is more likely in mitochondrial disorders. However, it is important to consider additional adaptive mechanisms to endurance exercise, such as angiogenesis, which can be modulated by mitochondria (54). These adaptions to central limitations are likely responsible for the increased exercise capacity in B6 control mice upon training since we did not find an increased oxidative capacity on the skeletal muscle level.

We performed both respirometry and RNASeq in the soleus muscle, which is an atypical muscle in mice due to a high percentage of type I fibers. We chose this muscle because mitochondrial mutations will mostly affect the oxidative type I fibers. In addition, the human muscles have a much higher percentage of type I fibers compared to mice, so the gene expression response of the soleus muscle in mice is the most comparable to human. Last, we focused on gene expression, which can be more responsive directly after an exercise stimulus. Thus, future studies correlating the proteome with exercise capacity and response might reveal additional determinants of exercise capacity.

Despite the significant variations in exercise response and determinants of exercise capacity with the mitochondrial mutations, we mostly found a positive exercise response with increased exercise capacity and reduced ROS production. This is in line with previous studies that reported beneficial effects of endurance exercise in the mitochondrial mutator mouse (55) and a complex I-deficient mouse model (56). It was shown that on the skeletal muscle level, mitochondrial function in mice translates well into humans (57). With respect to exercise physiology, humans are mostly limited by the oxygen transport to the muscles (central limitation), while mice are more limited by mitochondrial oxygen utilization (58, 59). However, in mitochondrial patients the mutations predominantly limit the mitochondrial oxygen utilization, thereby resulting in a shift toward a peripheral limitation of exercise capacity. This suggests that mice are valid models for the exercise adaptions in mitochondrial patients upon endurance exercise training and that endurance exercise might benefit patients with mitochondrial diseases. This is in line with a recent study that found an increased physical capacity in mitochondrial patients after an 8-wk exercise intervention (60).

Importantly, however, in ANT1 mice we found an aggravation of the preexisting, mild cardiomyopathy with endurance exercise. Endurance exercise can cause cardiac remodeling by volume overload, resulting in an increased LV diameter and increased wall thickness accompanied with a slight reduction in ejection fraction (61). This is known as athletes' heart and is often hard to distinguish from cardiomyopathy (62, 63). Exercised ANT1 mice do show LV dilation but no increase in wall thickness. In combination with the preexisting reduction in ejection fraction and the natural development of dilated cardiomyopathy with age (64), this indicates that the exercise-induced cardiac remodeling in ANT1 mice is pathologic rather than adaptive. Similarly, exercise-induced cardiomyopathy has been described in rats and humans but mostly for right ventricular dysfunction associated with ventricular arrhythmias (65, 66) or a higher prevalence of atrial fibrillation in endurance athletes (67). There has been no prior evidence that endurance exercise can worsen dilated cardiomyopathy. Mechanistically, the volume overload upon exercise could underlie the cardiac dilation in exercise-trained ANT1 mice. However, no LV dilation was observed in the other mitochondrial mutant mouse strains, suggesting an ANT1-specific mechanism. RNASeq indicated a role for stress response, immune system activation, and remodeling of electric coupling in the maladaptive response to exercise training in ANT1 mice, both of which have been described in cardiac remodeling upon exercise (68, 69). In contrast, we did not find an increase in the integrated stress response in skeletal muscle of ANT1 mice upon exercise training, suggesting no systemic stress or inflammatory response.

Current recommendations for patients with cardiomyopathy suggest moderate physical activity due to the cardiovascular benefits outweighing the increased risk of sudden cardiac deaths (70, 71). Here we revealed another risk factor in adverse cardiac remodeling of a mitochondrial cardiomyopathy upon endurance exercise.

Taken together, we demonstrated that endurance exercise is generally beneficial across different mitochondrial mutant mice, indicating its potential for PMD patients. In addition, we revealed that mitochondrial variations alter the exercise capacity, exercise response, and the determinants thereof, requiring personalized exercise recommendations in mitochondrial patients to avoid adverse events.

Materials and Methods

Mice. Five mouse strains were used for this study, all on the C57BL/6^{Eij} (Nnt$^{+/+}$) background: ND5 mice harboring the mtDNA mutation ND5 m.12352C > T (ND5^{S204F}), ND6 mice harboring the mtDNA mutation ND6 m.13997G > A

($ND6^{P25L}$), CO1 mice harboring the mtDNA mutation CO1m.6589T > C ($CO1^{V421A}$), ANT1 mice deficient for the nuclear-encoded adenine nucleotide translocator 1 (ANT1, $Slc25a4^{-/-}$) and harboring the ND5 m.12352C > T ($ND5^{S204F}$) mutation, and wild-type mice (B6). All mice were maintained on a 12:12 h light–dark cycle and fed 5LOD diet from PicoLab. The Institutional Animal Care and Use Committee from the Children's Hospital of Philadelphia approved all protocols, and the protocols comply with all relevant ethical regulations regarding animal research.

Study Design. Starting at the age of 16 wk, male mice were housed in the Comprehensive Lab Animal Monitoring System (CLAMS; Columbus Instruments) for 48 h to record their basal metabolism. After 2 d of recovery in their home cages, mice were subjected to an initial exercise stress test on a metabolic treadmill (Columbus Instruments) to assess their baseline exercise physiology. Two days later, half of the mice (selected randomly) started exercise training on an Exer 3/6 (Columbus Instruments). Exercise training consisted of running every second day for 45 min at 50% of the maximal step completed in the initial exercise stress test for a duration of 8 wk (28 training sessions). Nonexercised littermates were handled but were not run. Two days after the last training session, all mice were housed in the CLAMS again for 48 h. After 2 d of recovery in their home cages, mice performed an exercise stress test using the same protocol and performed at the same time of day as the initial test. After another 2 d of recovery in their home cages, echocardiography was performed on the mice, and mice were killed the same day within a time window of 4 h. Heart, gastrocnemius muscle, soleus muscle, tibialis anterior and extensor digitorum longus (EDL) muscles were flash frozen. From 1/4 of the mice, one gastrocnemius muscle was subjected to NADH Fluorescence Lifetime Imaging Microscopy (FLIM) measurements of the NAD+/NADH redox state, and from 3/4 of the mice, one soleus muscle was subjected to FluoRespirometry to assess skeletal muscle respiration. Mice were not fasted prior to any of the readouts or prior to being killed.

CLAMS. The CLAMS environmental chamber was set to 23 °C and a 12:12 light–dark cycle. The Oxymax (Columbus Instruments) was calibrated immediately prior to every measurement using a mix of 20.5% O_2 and 0.5% CO_2. Airflow was set to 0.5 L/min fresh air to each of the eight individual CLAMS cages. Mice were weighted and put in the CLAMS (Columbus Instrument) in the morning (10 AM to noon). Quantification of parameters started the following day with start of the light cycle at 7 AM and lasted for 24 h. Parameters quantified were VO_2, VCO_2, activity, running wheel activity, and food consumption at time intervals of ∼15 min for every mouse. This allowed calculation of the RER (VCO_2/VO_2) and energy expenditure [heat = (3.815 + 1.232 * RER) * VO_2].

Metabolic Treadmill. The Oxymax (Columbus Instruments) was calibrated once per day using a mix of 20.5% O_2 and 0.5% CO_2. Airflow was set to 0.5 L/min and the sampling interval to 5 s. The shock grid was set to shock intervals of 1/s and at the lowest shock intensity of 0.35 mA. The stepwise ramp protocol started with a 15-min acclimation period with the belt unmoving and the incline at 0°. The first step at 3 m/min was held for 5 min for the mouse getting used to the moving belt. From there, the speed was increased every 2 min to 5/7.5/10 m/min continuing in 2 m/min steps. At 12/16/20/26/30 m/min the speed was held for 4 min, and after the 2 min of the intervals, the incline of the treadmill was increased to 5/10/15/20/25°, respectively. Mice were run until exhaustion, which was defined as 5 consecutive seconds on the shock grid. Upon exhaustion, the belt was stopped and the shock grid turned off. Mice were kept another 12 min in the treadmill to record the recovery period. We chose this exercise stress test protocol with a relatively slow start and a faster ramp up of exercise intensity at 12 m/min through more frequent increase of incline to keep exercise time scales between ANT1 mice and the other mice as comparable as possible while maintaining enough differentiation to tease out the minor exercise intolerance of ND6 and CO1 mice.

Echocardiography. Echocardiography was performed using a Vevo2100 and a MS550D transducer (Visual Sonics). Mice were anesthetized with 3% isoflurane in 100% O_2, which was lowered to 1.5% during the procedure, targeting a heart rate of 450 bpm for the images. Average anesthesia length was ∼10 min per mouse. First, B-mode images of the parasternal long-axis view were taken, followed by B- and M-mode images of the parasternal short-axis view. For analysis, the LV trace function of VEVO LAB 3.2.6 (Visual Sonics) was used on the M-mode images of the parasternal short-axis view. To correct cardiac parameters for variations in heart rate, cardiac parameters of every mouse quantified at different heart rates were plotted over the heart rate. The resulting linear correlations for each strain were used to correct for the effects of differences in heart rate on cardiac parameters between individual mice.

FluoRespirometry. Mitochondrial respiration and ROS production in soleus muscle were assessed by the Oroboros Oxygraph-2K FluoRespirometer (Oroboros Instruments) as described previously (72). The Oroboros Oxygraph-2k was first calibrated to air with Mir05Cr respiratory buffer (0.5 mM EGTA, 3 mM $MgCl_2$, 60 mM lactobionic acid, 20 mM taurine, 10 mM KH_2PO_4, 20 mM Hepes, 110 mM D-sucrose, and fatty acid-free BSA [1 g/L] with the addition of 20 mM creatine and 5 mM DTPA) using the following settings: block temperature, 37 °C; stirrer speed, 750 rpm; oxygen sensor gain, 2; data recording interval, 2 s; gain of fluorescence-module-green, 300. Calibration for ROS quantification was performed before the start of each respirometry run with the injection of 2 μL of 10 mM AmplexTM UltraRed (Thermo Fisher Scientific), 2 μL of peroxidase (500 U/mL), 2 μL of superoxide dismutase (5 U/mL), and calibration standards of 2 × 4 μL of 2.5 mM hydrogen peroxide. Additional calibrations using hydrogen peroxide were performed after the addition of the tissues and at the end of the measurement to account for a potential decrease in sensitivity.

Solei were dissected from mice and cut into four pieces, starting at the distal end. Each cut was perpendicular to the direction of the muscle fibers, allowing for permeabilization of the muscle fibers (validated by the absence of routine respiration before the addition of substrates). The resulting 2 × 2 pieces were weighed and suspended in Mir05Cr respiratory buffer, and two muscle pieces were added into each respiration chamber in 400 μL of Mir05Cr.

Substrates for mitochondrial respiration were added, and both respiration and ROS production were quantified after each addition. First, 5 μL of 2 M pyruvate, 2.5 μL of 400 mM malate, and 10 μL of 2 M glutamate were added, followed by 20 μL of 0.5 M adenosine diphosphate to measure complex I respiration. Addition of 20 μL of 1 M succinate provided OxPhos capacity. Then, 0.5 μL of 10 mM oligomycin was added to block complex V and determine leak respiration, followed by a titration of the uncoupler carbonyl cyanide-p-trifluoromethoxyphenylhydrazone (FCCP, 1 mM stock in 1-μL increments) to assess the ETS capacity. The chambers were reoxygenated prior to the addition of FCCP to avoid oxygen availability as a potential limiting factor. Five microliters of 1 mM rotenone was injected to ascertain complex II respiration. Finally, 2 μL of 5 mM antimycin A was added to assess nonmitochondrial background respiration, for which all other respiratory states were corrected. The chambers were reoxygenated again, providing a quantification of ROS production at the same respiratory state with two different oxygen concentrations. This allowed us to correct for the effect of oxygen levels on ROS production. In addition, ROS production after Antimycin A and upon ambient oxygen levels provided a surrogate marker for mitochondrial mass (*SI Appendix*, Fig. S12) due to homologation of mitochondrial ROS production in the presence of all uncouplers and inhibitors (5). Data were recorded and analyzed using DatLab7.

Citrate Synthase Activity. Flash-frozen gastrocnemius muscle was powdered using a mortar and pestle on dry ice. The powder was weighted and resuspended in homogenization buffer (50 mM triethanolamine, 1 mM EDTA) at 1:10 wt/vol and incubated for 15 min at 4 °C. Citrate synthase (CS) enzyme activity was determined by the change in absorbance of DTNB (Ellman's reagent) measured at 412 nm in kinetic mode. In a 96-well plate, 20 μL of CS assay mix (200 mM Tris, 10 mM acetyl-CoA, 10 mM DTNB, 10% Triton X-100), 7 μL of oxaloacetate (2 mM), and 10 μL of homogenate were added.

RNASeq.

Skeletal muscle. Sixty flash-frozen mouse soleus muscle samples, consisting of six non–exercise-trained, three exercise-trained responder, and three exercise-trained nonresponder samples for each of the five strains, i.e., B6 control, ND5, ND6, CO1, and ANT1, were sent to Genewiz for RNASeq using Poly-A-primers. Responders and nonresponders were selected as the highest (responders) or lowest (nonresponders) average fold change in VO_2max and running time upon exercise training. RNASeq fastq files were processed using the Spliced Transcripts Alignment to a Reference (STAR) alignment tool and subsequently normalized using the RNA-Seq by Expectation-Maximization (RSEM) package based upon the mm10 reference genome and the gencode version M17 gene annotation.

Quality control (QC) was performed by clustering all samples using principal component analysis (PCA).

Differential gene expression analysis was performed by comparing each gene in the exercise-trained vs. the non–exercise-trained group within each strain. The voom procedure was used to normalize the RSEM-generated expected counts followed by differential expression testing using R package limma to obtain *P* values and LogFC. Specifically, a total of 58,581 genes were tested for differential expression between the control and treatment samples. Pathway enrichment was performed using Gene Set Enrichment Analysis (GSEA) version 4.1.0 using a weighted scoring scheme and Hallmark and C2 CP gene sets. The same procedure of differential gene expression and pathway enrichment using GSEA was repeated for comparisons of 1) non–exercise-trained samples between each strain and 2) exercise-trained samples between each strain. In addition, enrichment analysis was performed in Metascape (73) between non–exercise-trained mutant strains versus non–exercise-trained B6 control (including genes with adjusted P value < 0.05) and between exercise-trained versus non–exercise-trained within each strain (including genes with nominal P value < 0.05).

Regression analysis was performed in order to find gene expression profiles associated with physiologic covariables within each strain and across all strains. Similarly, linear regression was also performed to find covariables associated with strain.

Next, we wanted to identify pathways enriched for the genes associated with select covariables like running time and VO_2max. The covariate analysis output was first split into positively correlated genes with estimate > 0 and negatively correlated genes with estimate < 0. Next, both lists were sorted by ascending P values and descending r-squared values. Sequential ranks were assigned from the most negatively correlated to the most positively correlated genes from low to high. Using the ranked covariate output, fGSEA (fast preranked gene set enrichment analysis) analysis was performed using the R package fgsea. This process was repeated for running time, VO_2max, delta running time (improvement in running time by exercise training, in exercise-trained mice only), and delta VO_2max (improvement in VO_2max by exercise training, in exercise-trained mice only) for each of the five strains as well as across all strains.

Heart. Sixty flash-frozen mouse heart samples, consisting of six non–exercise-trained, three exercise-trained responder, and three exercise-trained nonresponder samples for each of the five strains, i.e., B6 control, ND5, ND6, CO1, and ANT1 were sent to Genewiz for RNASeq using Poly-A-primers. RNASeq fastq files were processed using the STAR alignment tool and subsequently normalized using the RSEM package based upon the mm10 reference genome and the gencode version M17 gene annotation.

QC was performed by clustering all samples using PCA.

Differential gene expression analysis was performed by comparing each gene in the exercised vs. the nonexercised group within each strain. The voom procedure was used to normalize the RSEM-generated expected counts followed by differential expression testing using R package limma to obtain *P* values and LogFC. Specifically, a total of 58,581 genes were tested for differential expression between the control and treatment samples. Pathway enrichment was performed using GSEA version 4.1.0 using a weighted scoring scheme and Hallmark and C2 CP gene sets. The same procedure of differential gene expression and pathway enrichment using GSEA was repeated for comparisons of 1) non–exercise-trained samples between each strain and 2) exercise-trained samples between each strain.

Regression analysis was performed in order to find gene expression profiles associated with physiologic covariables within each strain and across all strains. Similarly, linear regression was also performed to find covariables associated with strain.

Next, we wanted to get pathways enriched for the genes associated with select covariables like LV diameter, stroke volume, ejection fraction, fractional shortening, LV mass, LV anterior wall thickness, and LVPW thickness for each of the five strains as well as across all strains. The covariate analysis output was first split into positively correlated genes with estimate > 0 and negatively correlated genes with estimate < 0. Next, both lists were sorted by ascending P values and descending r-squared values. Sequential ranks were assigned from the most negatively correlated to the most positively correlated genes from low to high. Using the ranked covariate output, fGSEA analysis was performed using the R package fgsea.

Code is available via GitHub (https://github.com/komalsrathi/skeletal-muscle-rnaseq).

The raw and processed RNASeq data have been deposited at NCBI's Gene Expression Omnibus (GEO) and are accessible through GEO Series accession no. GSE198229 (https://www.ncbi.nlm.nih.gov/geo/query/acc.cgi?acc=GSE198229).

Differential gene expression and GSEA results are attached to this publication as supporting datasets (Datasets S1–S11).

Statistics. Gaussian distributions of the data were checked using a D'Agostino and Pearson omnibus normality test (significance level $\alpha < 0.05$). If the normality test was passed, a two-tailed *t* test or a one-way ANOVA with Bonferroni correction for multiple testing was performed; if the normality test failed, a Mann–Whitney test or Kruskal–Wallis test with Dunn's multiple comparison tests was used.

The effects of exercise training in tests that were performed before and after training are displayed as fold change normalized to nonexercised (rested) and calculated as

$$(\text{exercised}_{\text{post}}/\text{exercised}_{\text{prior}})/(\text{rested}_{\text{post}}/\text{rested}_{\text{prior}}).$$

This normalization was performed to correct for potential change in the parameters with age in the nonexercised cohort. Significances between strains were indicated graphically as asterisks and between exercised and rested as # (*$P < 0.05$, $^{\#}P < 0.05$, **$P < 0.01$, $^{\#\#}P < 0.01$, ***$P < 0.001$, $^{\#\#\#}P < 0.001$).

Statistics for RNASeq are described in *RNASeq*.

Data Availability. Code is available via GitHub (https://github.com/komalsrathi/skeletal-muscle-rnaseq). RNASeq data have been deposited in GEO (accession no. GSE198229) (74).

All other study data are included in the article and/or supporting information.

ACKNOWLEDGMENTS. This work was supported by the German Research Foundation (Grant SCHA 2182/1-1) to P.M.S. and NIH grants NS021328, MH108592, and OD010944 plus US Department of Defense grants W81XWH-16-1-0401 and W81XWH-21-1-0128 (PR202887.e002) awarded to D.C.W. Schematics were created with BioRender.com.

Author affiliations: [a]Center for Mitochondrial and Epigenomic Medicine, Division of Human Genetics, Department of Pediatrics, Children's Hospital of Philadelphia, Philadelphia, PA 19104; [b]Department of Biomedical Informatics, Children's Hospital of Philadelphia, Philadelphia, PA 19104; and [c]Department of Pediatrics, Perelman School of Medicine, University of Pennsylvania, Philadelphia, PA 19104

1. D. C. Wallace, A mitochondrial bioenergetic etiology of disease. *J. Clin. Invest.* **123**, 1405–1412 (2013).
2. D. C. Wallace, Genetics: Mitochondrial DNA in evolution and disease. *Nature* **535**, 498–500 (2016).
3. E. Malfatti *et al.*, Novel mutations of ND genes in complex I deficiency associated with mitochondrial encephalopathy. *Brain* **130**, 1894–1904 (2007).
4. C. S. Lin *et al.*, Mouse mtDNA mutant model of Leber hereditary optic neuropathy. *Proc. Natl. Acad. Sci. U.S.A.* **109**, 20065–20070 (2012).
5. T. Yardeni *et al.*, An mtDNA mutant mouse demonstrates that mitochondrial deficiency can result in autism endophenotypes. *Proc. Natl. Acad. Sci. U.S.A.* **118**, e2021429118 (2021).
6. A. Angelin *et al.*, Foxp3 reprograms T cell metabolism to function in low-glucose, high-lactate environments. *Cell Metab.* **25**, 1282–1293 (2017).
7. W. Fan *et al.*, A mouse model of mitochondrial disease reveals germline selection against severe mtDNA mutations. *Science* **319**, 958–962 (2008).
8. K. A. Strauss *et al.*, Severity of cardiomyopathy associated with adenine nucleotide translocator-1 deficiency correlates with mtDNA haplogroup. *Proc. Natl. Acad. Sci. U.S.A.* **110**, 3453–3458 (2013).
9. L. Palmieri *et al.*, Complete loss-of-function of the heart/muscle-specific adenine nucleotide translocator is associated with mitochondrial myopathy and cardiomyopathy. *Hum. Mol. Genet.* **14**, 3079–3088 (2005).
10. A. Echaniz-Laguna *et al.*, Complete loss of expression of the ANT1 gene causing cardiomyopathy and myopathy. *J. Med. Genet.* **49**, 146–150 (2012).
11. B. H. Graham *et al.*, A mouse model for mitochondrial myopathy and cardiomyopathy resulting from a deficiency in the heart/muscle isoform of the adenine nucleotide translocator. *Nat. Genet.* **16**, 226–234 (1997).
12. R. M. Morrow *et al.*, Mitochondrial energy deficiency leads to hyperproliferation of skeletal muscle mitochondria and enhanced insulin sensitivity. *Proc. Natl. Acad. Sci. U.S.A.* **114**, 2705–2710 (2017).
13. V. Subramaniam *et al.*, MITOCHIP assessment of differential gene expression in the skeletal muscle of Ant1 knockout mice: Coordinate regulation of OXPHOS, antioxidant, and apoptotic genes. *Biochim. Biophys. Acta* **1777**, 666–675 (2008).
14. J. E. Kokoszka *et al.*, The ADP/ATP translocator is not essential for the mitochondrial permeability transition pore. *Nature* **427**, 461–465 (2004).

15. J. Karch *et al.*, Inhibition of mitochondrial permeability transition by deletion of the ANT family and CypD. *Sci. Adv.* **5**, eaaw4597 (2019).
16. A. M. Bertholet *et al.*, H^+ transport is an integral function of the mitochondrial ADP/ATP carrier. *Nature* **571**, 515–520 (2019).
17. A. Hoshino *et al.*, The ADP/ATP translocase drives mitophagy independent of nucleotide exchange. *Nature* **575**, 375–379 (2019).
18. E. Ruiz-Pesini, D. Mishmar, M. Brandon, V. Procaccio, D. C. Wallace, Effects of purifying and adaptive selection on regional variation in human mtDNA. *Science* **303**, 223–226 (2004).
19. D. C. Wallace, Mitochondrial DNA variation in human radiation and disease. *Cell* **163**, 33–38 (2015).
20. S. Bertram, K. Brixius, C. Brinkmann, Exercise for the diabetic brain: How physical training may help prevent dementia and Alzheimer's disease in T2DM patients. *Endocrine* **53**, 350–363 (2016).
21. E. Barbieri *et al.*, The pleiotropic effect of physical exercise on mitochondrial dynamics in aging skeletal muscle. *Oxid. Med. Cell. Longev.* **2015**, 917085 (2015).
22. T. D. Jeppesen *et al.*, Aerobic training is safe and improves exercise capacity in patients with mitochondrial myopathy. *Brain* **129**, 3402–3412 (2006).
23. M. A. Tarnopolsky, Exercise as a therapeutic strategy for primary mitochondrial cytopathies. *J. Child Neurol.* **29**, 1225–1234 (2014).
24. J. L. Gardner, L. Craven, D. M. Turnbull, R. W. Taylor, Experimental strategies towards treating mitochondrial DNA disorders. *Biosci. Rep.* **27**, 139–150 (2007).
25. C. Cantó *et al.*, Interdependence of AMPK and SIRT1 for metabolic adaptation to fasting and exercise in skeletal muscle. *Cell Metab.* **11**, 213–219 (2010).
26. A. T. White, S. Schenk, NAD(+)/NADH and skeletal muscle mitochondrial adaptations to exercise. *Am. J. Physiol. Endocrinol. Metab.* **303**, E308–E321 (2012).
27. A. Thirupathi, C. T. de Souza, Multi-regulatory network of ROS: The interconnection of ROS, PGC-1 alpha, and AMPK-SIRT1 during exercise. *J. Physiol. Biochem.* **73**, 487–494 (2017).
28. B. A. Irving *et al.*, Combined training enhances skeletal muscle mitochondrial oxidative capacity independent of age. *J. Clin. Endocrinol. Metab.* **100**, 1654–1663 (2015).
29. R. A. Scott *et al.*, Mitochondrial haplogroups associated with elite Kenyan athlete status. *Med. Sci. Sports Exerc.* **41**, 123–128 (2009).
30. M. Deason *et al.*, Importance of mitochondrial haplotypes and maternal lineage in sprint performance among individuals of West African ancestry. *Scand. J. Med. Sci. Sports* **22**, 217–223 (2012).
31. A. K. Niemi, K. Majamaa, Mitochondrial DNA and ACTN3 genotypes in Finnish elite endurance and sprint athletes. *Eur. J. Hum. Genet.* **13**, 965–969 (2005).
32. A. Maruszak *et al.*, Mitochondrial DNA variation is associated with elite athletic status in the Polish population. *Scand. J. Med. Sci. Sports* **24**, 311–318 (2014).
33. G. Nogales-Gadea *et al.*, Are mitochondrial haplogroups associated with elite athletic status? A study on a Spanish cohort. *Mitochondrion* **11**, 905–908 (2011).
34. E. Mikami *et al.*, Comprehensive analysis of common and rare mitochondrial DNA variants in elite Japanese athletes: A case-control study. *J. Hum. Genet.* **58**, 780–787 (2013).
35. K. C. Kim, H. I. Cho, W. Kim, MtDNA haplogroups and elite Korean athlete status. *Int. J. Sports Med.* **33**, 76–80 (2012).
36. C. Bouchard *et al.*, Adverse metabolic response to regular exercise: Is it a rare or common occurrence? *PLoS One* **7**, e37887 (2012).
37. T. N. Mann, R. P. Lamberts, M. I. Lambert, High responders and low responders: Factors associated with individual variation in response to standardized training. *Sports Med.* **44**, 1113–1124 (2014).
38. C. Bouchard *et al.*, Genomic predictors of the maximal O2 uptake response to standardized exercise training programs. *J. Appl. Physiol. (1985)* **110**, 1160–1170 (2011).
39. T. Rankinen *et al.*, The Na(+)-K(+)-ATPase alpha2 gene and trainability of cardiorespiratory endurance: The HERITAGE family study. *J. Appl. Physiol. (1985)* **88**, 346–351 (2000).
40. A. Zarebska *et al.*, The GSTP1 c.313A>G polymorphism modulates the cardiorespiratory response to aerobic training. *Biol. Sport* **31**, 261–266 (2014).
41. J. A. McKenzie, S. Witkowski, A. T. Ludlow, S. M. Roth, J. M. Hagberg, AKT1 G205T genotype influences obesity-related metabolic phenotypes and their responses to aerobic exercise training in older Caucasians. *Exp. Physiol.* **96**, 338–347 (2011).
42. S. Onkelinx *et al.*, The CAREGENE study: Genetic variants of the endothelium and aerobic power in patients with coronary artery disease. *Acta Cardiol.* **66**, 407–414 (2011).
43. Z. He *et al.*, NRF-1 genotypes and endurance exercise capacity in young Chinese men. *Br. J. Sports Med.* **42**, 361–366 (2008).
44. L. Pérusse *et al.*, Familial aggregation of submaximal aerobic performance in the HERITAGE Family study. *Med. Sci. Sports Exerc.* **33**, 597–604 (2001).
45. F. T. Dionne *et al.*, Mitochondrial DNA sequence polymorphism, VO2max, and response to endurance training. *Med. Sci. Sports Exerc.* **23**, 177–185 (1991).
46. H. Murakami *et al.*, Polymorphisms in control region of mtDNA relates to individual differences in endurance capacity or trainability. *Jpn. J. Physiol.* **52**, 247–256 (2002).
47. J. A. Sanford *et al.*; Molecular Transducers of Physical Activity Consortium, Molecular Transducers of Physical Activity Consortium (MoTrPAC): Mapping the dynamic responses to exercise. *Cell* **181**, 1464–1474 (2020).
48. J. M. Robbins *et al.*, Human plasma proteomic profiles indicative of cardiorespiratory fitness. *Nat. Metab.* **3**, 786–797 (2021).
49. S. Martinez-Huenchullan, S. V. McLennan, A. Verhoeven, S. M. Twigg, C. S. Tam, The emerging role of skeletal muscle extracellular matrix remodelling in obesity and exercise. *Obes. Rev.* **18**, 776–790 (2017).
50. M. Kjaer *et al.*, Extracellular matrix adaptation of tendon and skeletal muscle to exercise. *J. Anat.* **208**, 445–450 (2006).
51. J. A. Timmons *et al.*, Modulation of extracellular matrix genes reflects the magnitude of physiological adaptation to aerobic exercise training in humans. *BMC Biol.* **3**, 19 (2005).
52. W. Zhang, Y. Liu, H. Zhang, Extracellular matrix: An important regulator of cell functions and skeletal muscle development. *Cell Biosci.* **11**, 65 (2021).
53. C. J. Williams *et al.*, Genes to predict VO_{2max} trainability: A systematic review. *BMC Genomics* **18** (suppl. 8), 831 (2017).
54. A. Reichard, K. Asosingh, The role of mitochondria in angiogenesis. *Mol. Biol. Rep.* **46**, 1393–1400 (2019).
55. A. Safdar *et al.*, Endurance exercise rescues progeroid aging and induces systemic mitochondrial rejuvenation in mtDNA mutator mice. *Proc. Natl. Acad. Sci. U.S.A.* **108**, 4135–4140 (2011).
56. C. Fiuza-Luces *et al.*, Physical exercise and mitochondrial disease: Insights from a mouse model. *Front. Neurol.* **10**, 790 (2019).
57. R. A. Jacobs, V. Díaz, A. K. Meinild, M. Gassmann, C. Lundby, The C57Bl/6 mouse serves as a suitable model of human skeletal muscle mitochondrial function. *Exp. Physiol.* **98**, 908–921 (2013).
58. D. Montero *et al.*, Haematological rather than skeletal muscle adaptations contribute to the increase in peak oxygen uptake induced by moderate endurance training. *J. Physiol.* **593**, 4677–4688 (2015).
59. B. M. Gabriel, J. R. Zierath, The limits of exercise physiology: From performance to health. *Cell Metab.* **25**, 1000–1011 (2017).
60. C. Fiuza-Luces *et al.*, Health benefits of an innovative exercise program for mitochondrial disorders. *Med. Sci. Sports Exerc.* **50**, 1142–1151 (2018).
61. T. Luijkx *et al.*, Sport category is an important determinant of cardiac adaptation: An MRI study. *Br. J. Sports Med.* **46**, 1119–1124 (2012).
62. M. J. Brosnan, D. Rakhit, Differentiating athlete's heart from cardiomyopathies–The left side. *Heart Lung Circ.* **27**, 1052–1062 (2018).
63. M. Abulí, M. S. de la Garza, M. Sitges, Differentiating athlete's heart from left ventricle cardiomyopathies. *J. Cardiovasc. Transl. Res.* **13**, 265–273 (2020).
64. N. Narula *et al.*, Adenine nucleotide translocase 1 deficiency results in dilated cardiomyopathy with defects in myocardial mechanics, histopathological alterations, and activation of apoptosis. *JACC Cardiovasc. Imaging* **4**, 1–10 (2011).
65. B. Benito *et al.*, Cardiac arrhythmogenic remodeling in a rat model of long-term intensive exercise training. *Circulation* **123**, 13–22 (2011).
66. A. La Gerche *et al.*, Exercise-induced right ventricular dysfunction and structural remodelling in endurance athletes. *Eur. Heart J.* **33**, 998–1006 (2012).
67. K. Andersen *et al.*, Risk of arrhythmias in 52 755 long-distance cross-country skiers: A cohort study. *Eur. Heart J.* **34**, 3624–3631 (2013).
68. R. B. Vega, J. P. Konhilas, D. P. Kelly, L. A. Leinwand, Molecular mechanisms underlying cardiac adaptation to exercise. *Cell Metab.* **25**, 1012–1026 (2017).
69. B. C. Bernardo, J. R. McMullen, Molecular aspects of exercise-induced cardiac remodeling. *Cardiol. Clin.* **34**, 515–530 (2016).
70. J. Basu, A. Malhotra, M. Papadakis, Exercise and hypertrophic cardiomyopathy: Two incompatible entities? *Clin. Cardiol.* **43**, 889–896 (2020).
71. Y. G. Seo *et al.*, What is the optimal exercise prescription for patients with dilated cardiomyopathy in cardiac rehabilitation? A systematic review. *J. Cardiopulm. Rehabil. Prev.* **39**, 235–240 (2019).
72. T. Komlódi *et al.*, Comparison of mitochondrial incubation media for measurement of respiration and hydrogen peroxide production. *Methods Mol. Biol.* **1782**, 137–155 (2018).
73. Y. Zhou *et al.*, Metascape provides a biologist-oriented resource for the analysis of systems-level datasets. *Nat. Commun.* **10**, 1–10 (2019).
74. P. M. Schaefer *et al.*, Mitochondrial mutations alter endurance exercise response and determinants in mice. Gene Expression Omnibus (GEO). https://www.ncbi.nlm.nih.gov/geo/query/acc.cgi?acc=GSE198229. Deposited 9 March 2022.